ARTICLE NO. 78-502R

Visualization of Quasiperiodic Flows

Robert A. Kadlec*
University of Colorado, Boulder, Colo.
and
Sanford S. Davis†
NASA Ames Research Center, Moffett Field, Calif.

A self-synchronizing Schlieren flow visualization technique has been developed to study unsteady periodic flows that may result from aeroelastic effects. The technique allows the experimentalist to stroboscopically "freeze" the streak line pattern at any phase in one period of the motion by driving the Schlieren light source with an electronically processed synchronizing signal that is derived by measuring a periodic flow variable with a convenient sensor. Results for the visualization of the near wake behind an oscillating airfoil at low speeds, which show an ordered series of discrete vortices and a curious short-wavelength wake disturbance are examined. Results are also presented for edge tone sound generation.

Nomenclature

a = pitch amplitude at trailing edge
a/c = pitch amplitude ratio
c = airfoil chord
d = edge tone channel width
f = edge tone sound frequency
h = edge tone edge distance
k = reduced frequency, $\omega c/2U_\infty$
Re_c = Reynolds number based on airfoil chord
Re_d = Reynolds number based on edge tone channel width
Re_δ = Reynolds number based on boundary-layer displacement thickness
U_∞ = freestream velocity
v_{te} = airfoil trailing-edge vertical velocity, $\dot{y}_{te}$
y_{te} = airfoil trailing-edge vertical displacement
α = wake disturbance wave number, $2\pi/\lambda$

Introduction

UNSTEADY aerodynamics includes many examples of fundamental interest having the common characteristic that the flow variables change periodically with time over a large portion of the flow but often with a frequency that drifts; that is, the flow is quasiperiodic. In some cases this periodicity is the consequence of rotating or oscillating surfaces in the flow. Representatives of this class occur in the aerodynamics of rotorcraft and in important aeroelastic effects such as flutter at transonic speeds. In other cases flow instabilities themselves lead to periodic disturbances while the solid surfaces in the flow remain fixed. This class includes many important aeroacoustic flows such as noise generation from vortex shedding and from the interaction of jets, wakes, and vortices with rigid surfaces.

Often insight about flow behavior may be gained when a pattern produced by or related to the flow can be observed by visual inspection. This is especially true for unsteady flows for which knowledge of the flow development and evolution is important. In order to visualize an unsteady flow, however, special schemes must be adopted to enable the experimentalist to resolve the temporal behavior of the flow. This study has concentrated on the development and assessment of a special flow visualization technique that may be used to investigate quasiperiodic flows.

Conventionally, the visualization of unsteady flows is accomplished by using single-shot and multishot spark flash photography and high-speed cinematography.[1] When the unsteady flow is also periodic, the visualization apparatus may include a pulsed light source in which the pulses can be made to coincide with the instants at which successive occurrences of the phenomenon being studied reach a fixed geometrical position. The overall result produces a stroboscopic effect, creating the illusion that the unsteady motion has stopped at one instant in the period of motion. In common practice the strobe light source, driven by an independent frequency source, is set at a frequency approximately equal to that of the periodic phenomenon under investigation; it is, in other words, fixed-frequency stroboscopy.[2] However, in unsteady aerodynamic experiments small but uncontrollable changes in experimental conditions invariably cause the flowfield frequency to drift. As a result, all of the unsteady techniques mentioned are limited in their capacity to capture a flow image at a precise phase in the motion. As a matter of fact, phase uncertainty can be so large that no visual continuity may be obtained. This difficulty can be overcome by synchronizing the light source flashes with the quasiperiodic flow itself. Although synchronization can be used with spark flash photography and high-speed cinematography, in the present application we have adapted it to a Schlieren visualization technique that synchronizes a stroboscopic light source with the quasiperiodic flow. In this way the technique enables the experimentalist to visualize the detailed space-time behavior of a quasiperiodic flow while the experiment is in progress.

Self-Synchronizing Stroboscopic Schlieren System

An early version of a stroboscopic Schlieren system which used synchronization to cope with fluctuating frequency phenomena was developed by Lawrence[3] at the NASA Ames Research Center and was used in a limited application to visualize the vortex discharge behind blunt trailing-edge airfoils. The present system is based on the Lawrence design but also incorporates several design changes and some

Presented as Paper 78-502 at the AIAA/ASME 19th Structures, Structural Dynamics and Materials Conference, Bethesda, Md., April 3-5, 1978; submitted June 1, 1978; revision received March 30, 1979.

Index categories: Aeroacoustics; Nonsteady Aerodynamics; Aeroelasticity and Hydroelasticity.
*Assistant Professor, Dept. of Aerospace Engineering Sciences. Member AIAA.
†Research Scientist. Member AIAA.

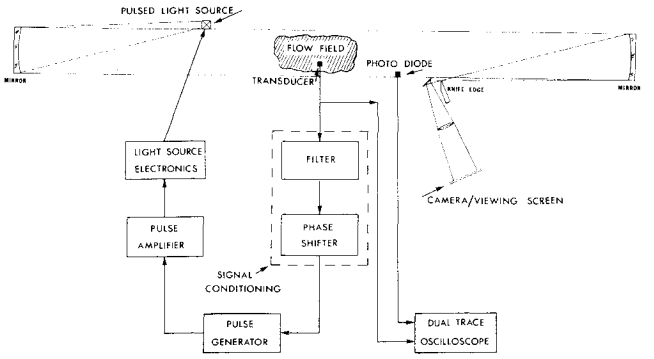

Fig. 1 Schematic diagram of self-synchronizing stroboscopic Schlieren system.

modern improvements. The important components of this system are diagrammed schematically in Fig. 1.

Perhaps the best way to understand the operation of this system is to follow a synchronizing signal from its inception at the transducer to its conclusion at the pulsed light source. The synchronizing signal is derived by positioning a convenient transducer (pressure transducer, hot-wire anemometer, microphone, etc.) in the flowfield to measure a point variable with a periodic content. If, on the other hand, a flow in which solid surfaces are in motion is being studied, the synchronizing signal may be appropriately derived by measuring the motion of the solid surface. Both approaches were used in the applications presented. In addition to the periodic component, the total transducer signal contains a nonperiodic component, which should be viewed as noise and is caused by a variety of inputs such as intermittent turbulent bursts, turbulence, electronic pickup, etc. For the flows examined, this noise component is minimized by passing the transducer signal through a variable frequency bandpass filter. The clean synchronizing signal leaving the filter is fed into a phase-shift circuit which delays the signal by a known and controllable phase. This conditioned signal then drives a pulse generator and an amplifier, which in turn drives a mercury flash lamp that serves as the pulsed light source of a Toepler Schlieren system with concave spherical mirrors and a conventional Schlieren arrangement. The mercury flash lamp has a pulse duration of 25 μs, which sets an upper frequency limit of approximately 4000 Hz on the periodic flows, which can accurately be resolved without using a frequency division scheme. The large-diameter mirrors (0.45 m) allow observation of the global periodic flowfield. The image of the flowfield formed by the Schlieren system is recorded on a camera or viewing screen. A photodiode is mounted at the edge of the Schlieren field, and the output from this diode is compared with the transducer output on a dual-trace oscilloscope. This comparison measurement provides the experimentalist with an accurate display of the phase relationship between the stop-action view on the screen and the periodic transducer signal. In this way he is able to correlate the view of the flow with an important point flow variable. By viewing and photographically recording the motion at different phases, the experimentalist is able to reconstruct a high-speed periodic motion.

Applications

Visualization of the Near Wake Behind an Oscillating Airfoil

We first applied this system to the visualization of the near wake behind a pitching airfoil at low speeds. A knowledge about this flow is important for research work on flutter and also provides a check on theoretical assumptions made when estimating the unsteady aerodynamic loads on an oscillating airfoil. Our objective was to examine the structure of the wake at various frequencies and amplitudes.

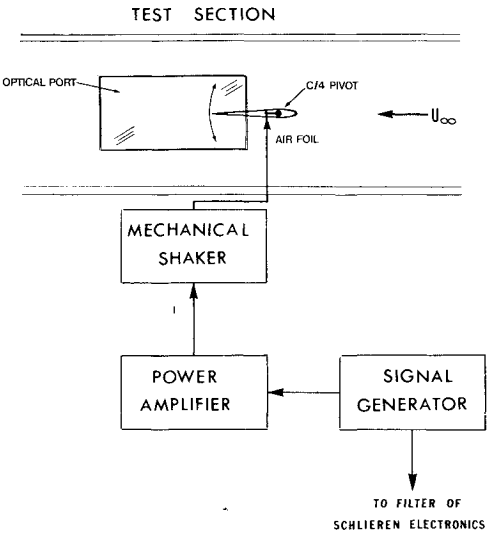

Fig. 2 Pitching airfoil experimental apparatus.

The experiment (Fig. 2) was performed in a 25- × 35-cm indraft wind tunnel fitted with optical ports. A 15-cm chord model of the NACA 64A006 laminar airfoil, mounted in the test section on pivots at its quarter chord, was positioned so that the trailing edge could be viewed at the side of the optical ports. The model was driven at frequencies of 40 and 60 Hz and pitch amplitude ratios a/c of 0.02 and 0.4. The tunnel speed was varied between approximately 3 and 10 m/s, resulting in a reduced frequency range k between 1 and 10. A phase-shifted signal derived from the signal generator was used to drive the shaker and the Schlieren system. The density gradients in the flow were artificially enhanced by heating a Ni-Cr wire embedded in the airfoil near the trailing edge.

Results

The stroboscopic Schlieren pictures, shown in Figs. 3-6 as a sequence of nine frames taken at 45-deg phase increments, are representative of the results obtained by the experiment. The 10-cm × 10-cm area shown in each photograph corresponds to the optical port dimensions. The trailing-edge velocity normalized by the freestream velocity is indicated under each frame. The ability of linearized unsteady airfoil theory to predict the unsteady loading can be correlated with the magnitude of this parameter. Figure 3 shows the unsteady wake for a reduced frequency k near 1.0. The calculated wavelength is 42 cm, so only a small portion of the wake disturbance is shown. Since wake distortion is small, it bears out the fundamental assumption of small disturbance theory that the wake is just a continuation of the airfoil chord line. This is further confirmed by the small values of the trailing-edge velocity ratios. However, the photographic evidence can be misleading. The results of recent pressure measurements on an oscillating airfoil by Satyanarayana and Davis[4] have shown that classical linear thin airfoil theory fails at $k \cong 0.6$ due to the failure of the Kutta-Joukouski condition.

Figure 4 depicts the unsteady wake behavior at a higher reduced frequency. The wake distortion is greater, and the larger trailing-edge velocity ratios indicate that the limits of small disturbance theory have already been exceeded. The wavelength based on the wake disturbance being convected is 13.7 cm, so about one half of the wave is visible in the pictures. The curious short-wave disturbance, most evident in frame 6, is a laminar wake instability wave. It will be described in more detail in a subsequent section. Figure 5 shows a similar case, in which the pitch amplitude ratio has been increased to 0.04. The effects are similar but magnified due to the greater excitation. Note that frames 1 and 9, which were taken at different times, indicate exactly the same flow pattern.

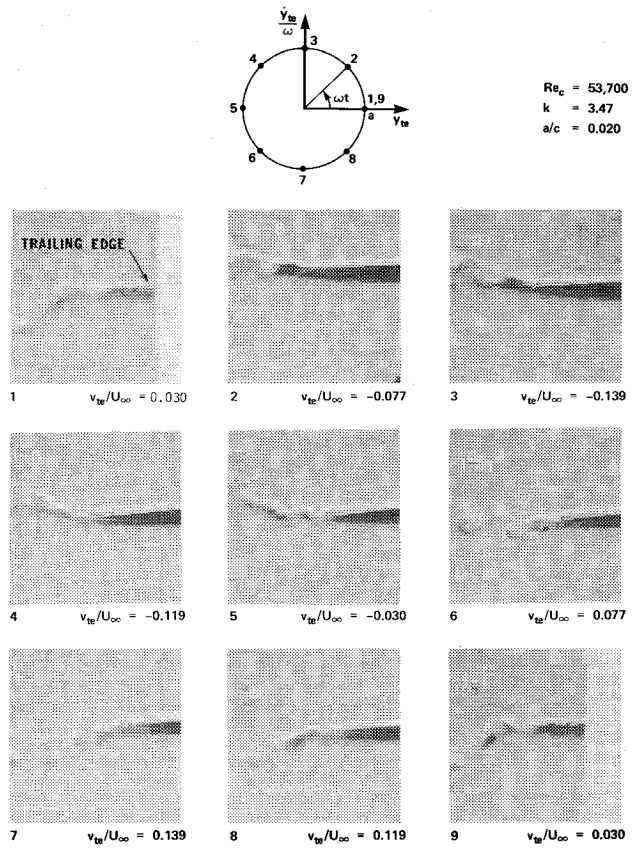

Fig. 3 Visualization of the near wake behind a pitching airfoil: $Re_c = 166{,}000$; $k = 1.12$; $a/c = 0.02$.

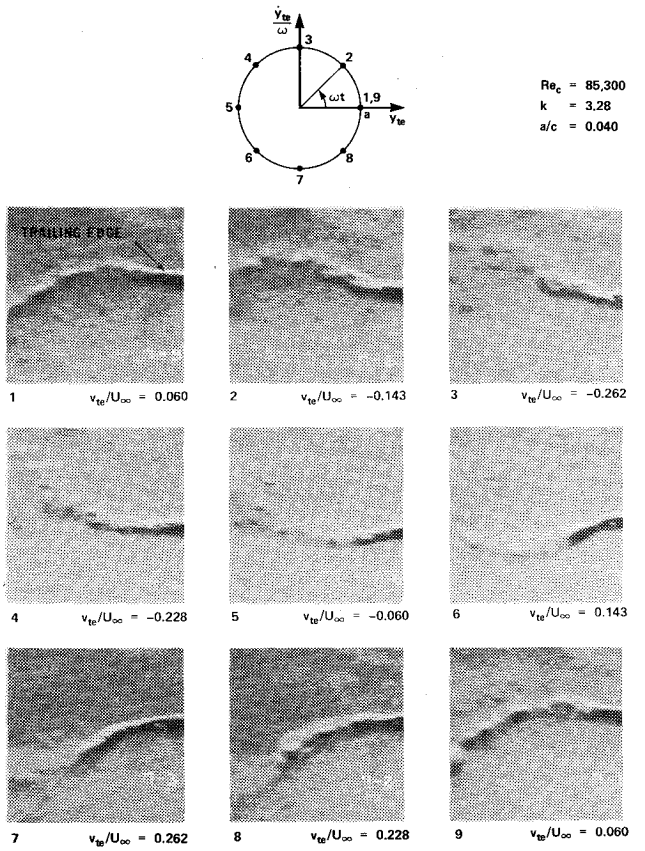

Fig. 4 Visualization of the near wake behind a pitching airfoil: $Re_c = 53{,}700$; $k = 3.47$; $a/c = 0.02$.

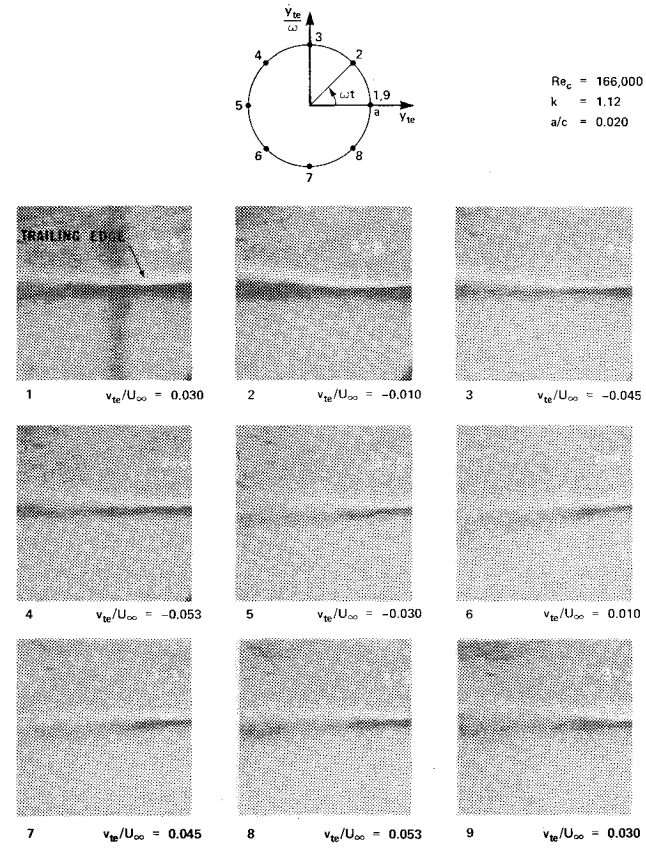

Fig. 5 Visualization of the near wake behind a pitching airfoil: $Re_c = 85{,}300$; $k = 3.28$; $a/c = 0.04$.

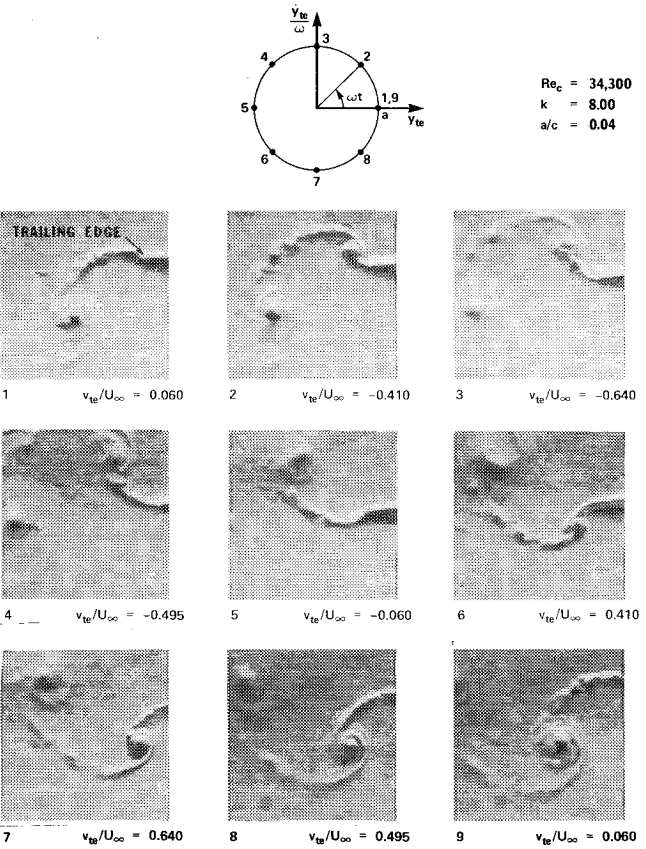

Fig. 6 Visualization of the near wake behind a pitching airfoil: $Re_c = 34{,}300$; $k = 8.00$; $a/c = 0.04$.

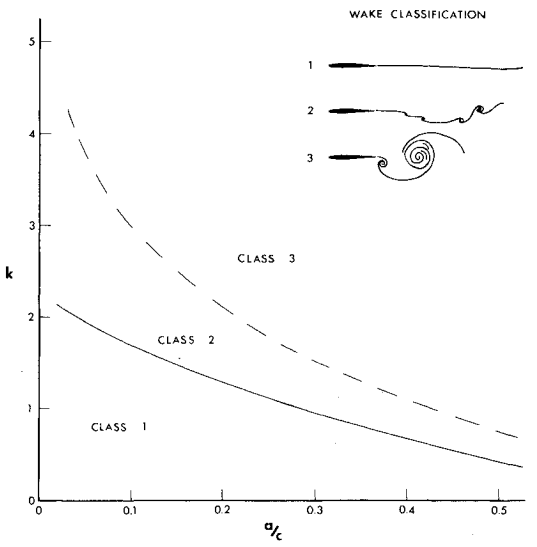

Fig. 7 Characterization of near-wake flow patterns.

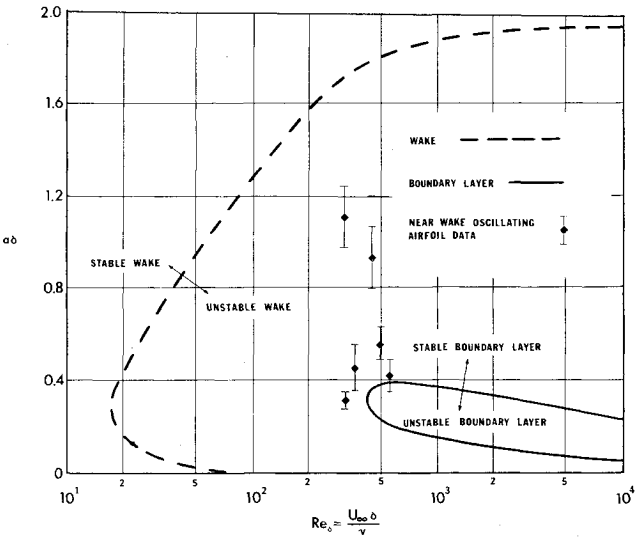

Fig. 8 Curves of neutral stability for near-wake flowfield.

Figure 6 shows an extreme example at very high reduced frequency. The wake excursion is so great that it becomes unstable and rolls up into itself, and the velocity ratios are so high that the flowfield is almost reminiscent of the flow broadside to a flat plate, as shown in the spark shadowgraphs of Pierce.[5] The calculated wavelength based on a convected disturbance is 5.9 cm.

All of the visualization photographs were used to classify the near wake according to the degree of wake distortion. Since the distortion is magnified by increasing either k or a/c, the classification is appropriately displayed on a k vs a/c graph (Fig. 7). The results show that the wake is characterized by three different classes that are separated by two boundary curves, where the boundary curves are described by an inverse relation between k and a/c. Class 1 includes wakes of small distortion where linearized unsteady airfoil theory applies, while class 2 describes those wakes that begin to break up into short-wavelength, vortex-like disturbances. Class 3 includes the extreme cases where the wake appears similar to that of vortex shedding. This classification confirms a previous visualization investigation by Ohashi and Ishikawa.[6]

Analysis of Instability Waves

According to the usual criteria, the boundary layer on this airfoil should remain laminar at the trailing edge. Once the boundary layer leaves the airfoil, the laminar wake is unstable and soon becomes turbulent. Figure 4, frame 6, shows the laminar boundary layer breaking up into a regular pattern. Traces of this regular pattern can also be seen in the other figures. These patterns are reminiscent of Tollmien-Schlicting waves on a wall boundary layer, photographic evidence of which was published by Burgh.[7]

In order to investigate the nature of these regular disturbance patterns, the wavelengths were measured from photographs and compared with classical linear stability theory. The stability theory adopted here assumes that the disturbance wave interacts with the mean flow in an unaccelerated flowfield. The disturbance stream function is found to satisfy the Orr-Sommerfeld equation with homogeneous boundary conditions. The behavior of the eigenvalues of this equation may be expressed by a neutral stability curve which separates exponentially growing disturbances from decaying disturbances.

The neutral curve is conventionally displayed as a graph of $\alpha\delta$ vs Re_δ, where $\alpha = 2\pi/\lambda$ is the wave number of the disturbance of wavelength λ; δ is the boundary-layer displacement thickness; and $Re_\delta = U_\infty \delta/\nu$. Usually neutral stability curves for boundary layers are displayed for two

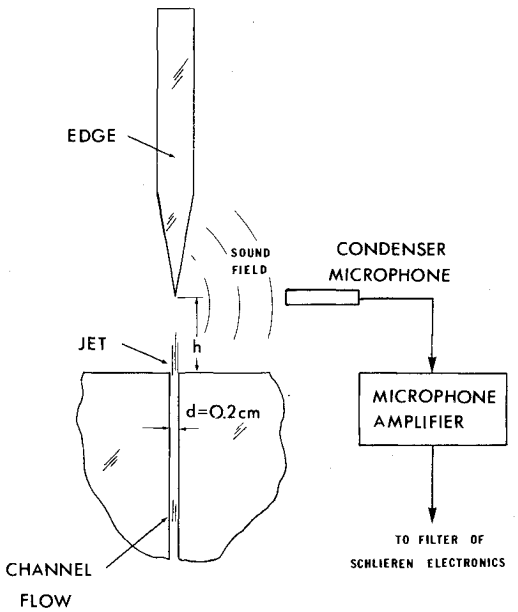

Fig. 9 Edge tone sound generation experimental apparatus.

choices of the mean velocity profile. For this experiment the Blasius profile was chosen as a model of the laminar boundary layer, and the resulting neutral stability curve attributed to Tollmien[8] was used. On the other hand, the velocity defect in the initially laminar wave was represented by an error function profile. The neutral stability curve calculated for this profile and given by Taneda[9] was used to describe the wake. Figure 8 shows both of these curves along with the experimental data. The graph is divided into three regions by the neutral stability curves: region I, where disturbances are unstable in both the boundary-layer region and the wake; region II, where disturbances are unstable in the wake only; and region III, where disturbances are unconditionally stable.

The conditions of the present experiment are not precisely those which are assumed by the traditional curves presented in Fig. 8. Aside from the fact that the boundary layer on the wing is accelerated and decelerated by the pressure gradients, the wing is being oscillated, so the basic flow itself is unsteady. An examination of the photographs shows that the disturbance scales in the wake due to the airfoil's oscillations are much larger than the instability scales, where the instability scale is one wavelength of an unstable wake

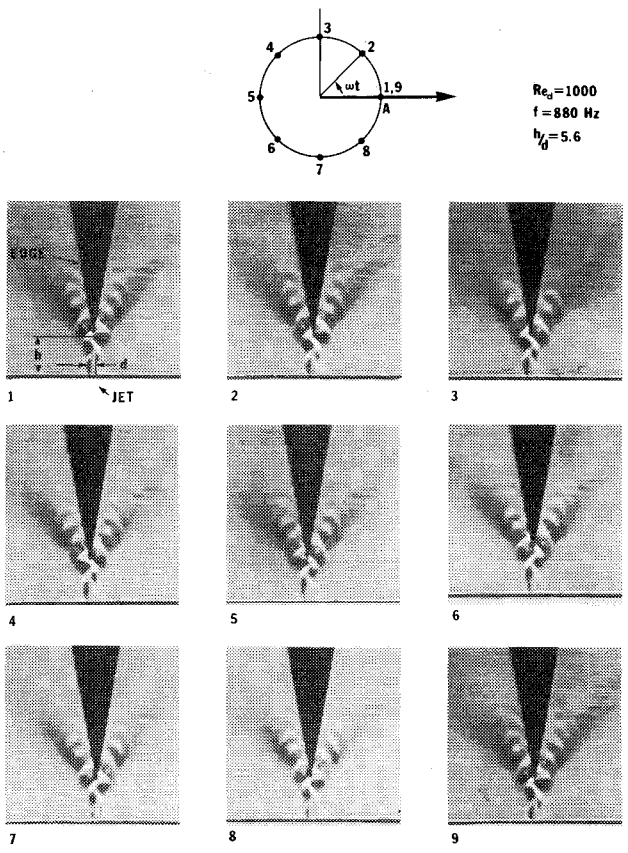

Fig. 10 Visualization of edge tone flowfield: $Re_d = 1000$; $f = 880$ Hz; $h/d = 5.6$.

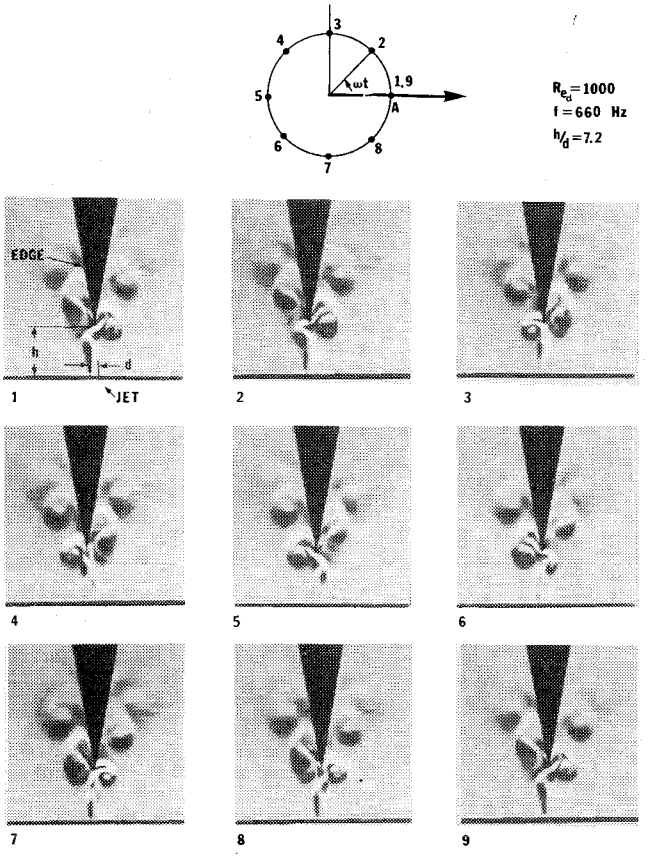

Fig. 11 Visualization of edge tone flowfield: $Re_d = 1000$; $f = 660$ Hz; $H/d = 7.2$.

disturbance. The disparity in scales indicates that the unsteady flow problem can probably be "uncoupled" from the stability problem. In this manner the measured wavelengths of the short-wave disturbances were considered to be the disturbance scales for the instability calculations. The value of δ was chosen as the calculated displacement thickness at the trailing edge and varied from 0.6 to 1.2 mm. All of the experimental data falls within region II, which indicates only a wake instability. These results indicate that the short-wave disturbances on the wake are probably laminar instability waves, similar to those in the shadowgraph photographs of Pierce.[5]

Edge Tone Sound Generation

To demonstrate the usefulness of the technique when oscillations in the flow are not the result of moving solids, we chose to visualize the edge tone flowfield. This old and thoroughly studied problem[10] is one example of an important larger class that is characterized by the production of sound through the interaction of shear layers with rigid surfaces. A diagram of the flow geometry is shown in Fig. 9. It is characterized by a thin laminar free jet which issues from a two-dimensional laminar channel flow of width d and impinges upon an edge aligned on the axis of the jet and displaced an edge distance h from the jet exit.

A striking feature of this flow occurs when the edge is withdrawn from the jet exit plane. When the edge distance reaches a minimum breadth, the device produces an audible tone. As the edge is removed further, the tone decreases in frequency as the inverse of distance h. This frequency decreases until a certain edge distance is reached, at which time the edge tone suddenly jumps to a new higher frequency or mode of operation. These features, together with several others, characterize this interesting phenomenon.

In order to visualize the periodic flowfield responsible for this sound, a condenser microphone was placed in the near sound field. The output from the microphone amplifier was fed into the filter input of the signal-conditioning electronics. After filtering the high frequencies (hiss) associated with the jet itself, a variable phase shift was introduced, whereupon the signal was fed into the pulse generator activating the Schlieren light source. In this way we were able to stroboscopically stop the edge tone flowfield at any phase in one period of the microphone signal.

Figures 10 and 11 are stroboscopic Schlieren pictures as a sequence of nine frames taken at 45-deg increments. Figure 10 shows the flowfield where the edge distance is slightly greater than the minimum breadth, while Fig. 11 captures the flow just before the frequency jumps to the next mode of operation.

Close inspection of these photographs reveals the detailed oscillations of the jet and the formation and growth of vortices on either side of the edge and their motion downstream. The patterns recorded in Fig. 11 indicated that the detailed features of the vortices leaving the edge may play a role in the transition to a higher mode.

Conclusions

We have found that the self-synchronizing stroboscopic Schlieren system visualization technique provides an extraordinarily effective means of studying quasiperiodic flows in real time. Based on the two applications just described, our experience indicates that this visualization system allows the experimentalist to examine patterns of a quasiperiodic motion at any phase in a cycle while the experiment is in progress. Also, the image on the viewing screen is a spatial signal average of the coherent periodic motion rather than a single realization, and this record results in a much higher signal-to-noise ratio since random components of the image cancel in the averaging process. Finally, the high-speed motion of a quasiperiodic flow can be reconstructed by recording photographs of the flow at different fixed time delays in one cycle. In order to record a meaningful stop-action view of the

flow, the basic flow requirements should be that 1) the size and shape of each disturbance must be nearly the same, and 2) the time history of each disturbance from a fixed point must be approximately constant for each cycle. Presently this technique is being extended to include self-synchronizing stroboscopic laser interferometry in order to make quantitative space-time density field measurements and to analyze unsteady flow around airfoils at transonic speeds.

References

[1] Merzkirch, W., *Flow Visualization*, Academic Press, New York, 1974.

[2] Edgerton, H. E., *Electronic Flash Strobe*, McGraw-Hill, New York, 1970.

[3] Lawrence, L. F, Schmidt, S. F., and Looschen, F. W., "A Self-Synchronizing Stroboscopic Schlieren System for the Study of Unsteady Air Flows," NACA TN 2509, 1951.

[4] Satyanarayana, B. and Davis, S., "Experimental Studies of Unsteady Trailing-Edge Conditions," *AIAA Journal* (to be published).

[5] Pierce, D., "Photographic Evidence of Formation and Growth of Vorticity Behind Plates Accelerated From Rest in Still Air," *Journal of Fluid Mechanics*, Vol. 11, Nov. 1961, p. 460.

[6] Ohashi, H. and Ishikawa, N., "Visualization Study of Flow Near the Trailing Edge of an Oscillating Airfoil," *Bulletin of the Japanese Society of Mechanical Engineers*, Vol. 15, July 1972, p. 840.

[7] Burgh, H., "A Method For Visualizing Boundary Layer Phenomena," *Proceedings of IUTAM Symposium on Boundary Layer Research*, Freiburg, Aug. 26-29, 1957, Springer-Verlag, Berlin, 1958.

[8] Schlicting, H., *Boundary Layer Theory*, 4th ed. McGraw-Hill, New York, 1960, p. 397.

[9] Taneda, S., "The Stability of Two-Dimensional Laminar Wakes at Low Reynolds Numbers," *Journal of the Physical Society of Japan*, Vol. 18, Feb. 1963, p. 288.

[10] Karamcheti, K., Bauer, A. B., Schields, W. L., Stegen, G. R., and Woolley, J. P., "Some Features of an Edge-Tone Flow Field," *Basic Aerodynamic Noise Research*, edited by I. R. Schwarz, NASA SP-207, 1969.